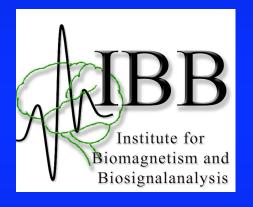
Reconstruction and manipulation of neuronal networks in the human brain



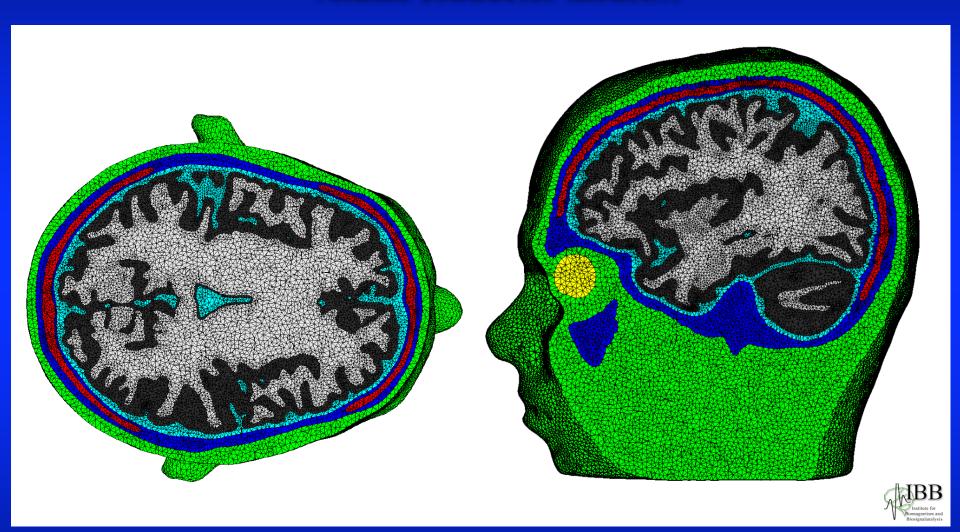


Carsten H. Wolters

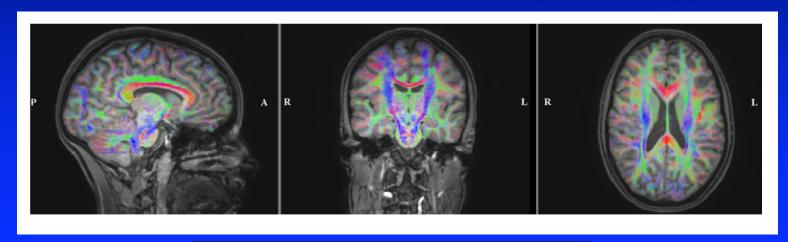
Outline

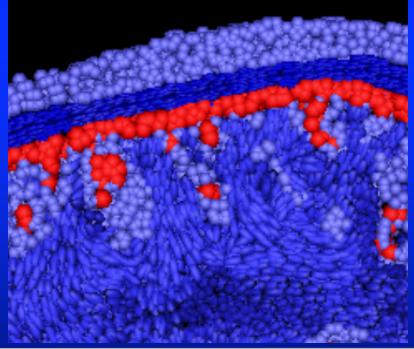
- Head model generation: MRI/DTI registration and segmentation and individual modeling of head tissue conductivities
- Forward modeling in TES and EEG: Numerical investigations
- Reconstruction: Combined EEG/MEG source analysis in presurgical epilepsy diagnosis
- Manipulation: Optimization approaches for multi-sensor tES/TMS and application to the individual stimulation of the somatosensory cortex
- Summary

Goal: Calibrated realistic finite element method (FEM) head volume conductor model...



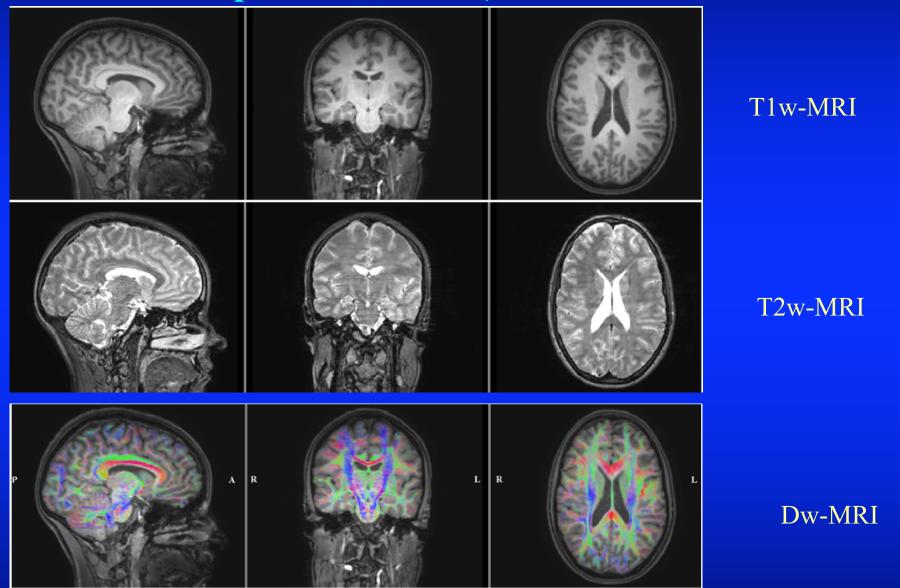
...with white matter conductivity anisotropy





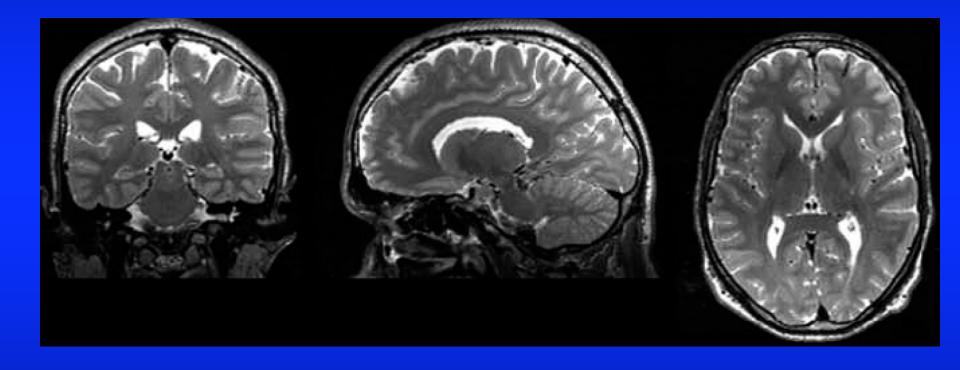
carsten.wolters@uni-muenster.de

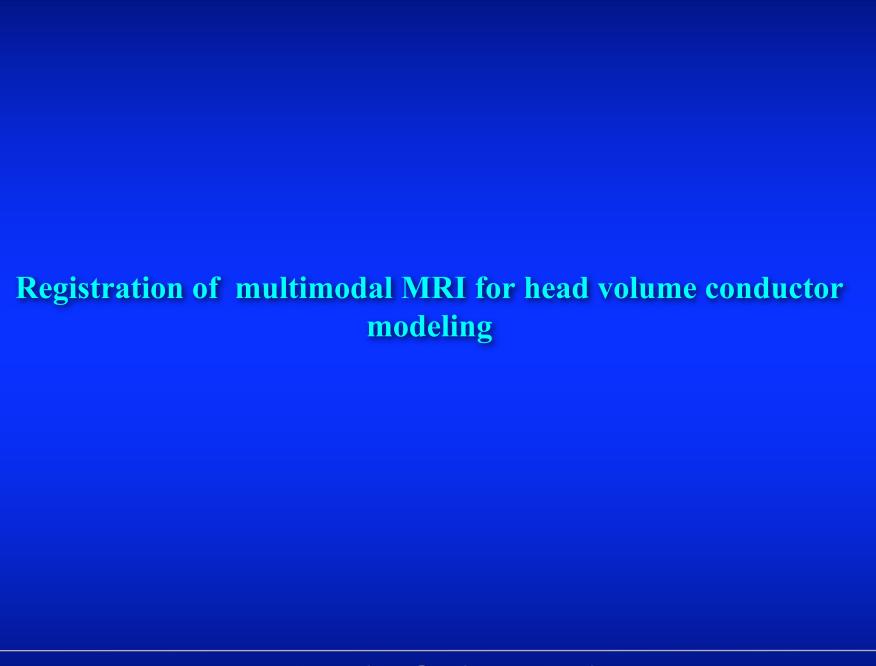
Recommended input: MRI data (27 min measurement time)



carsten.wolters@uni-muenster.de

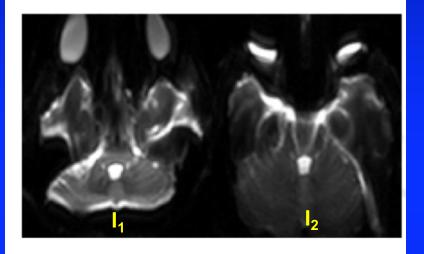
Why T2-MRI: Good basis for segmentation of CSF and skull

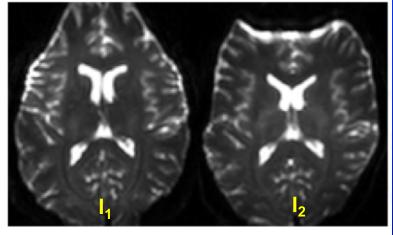


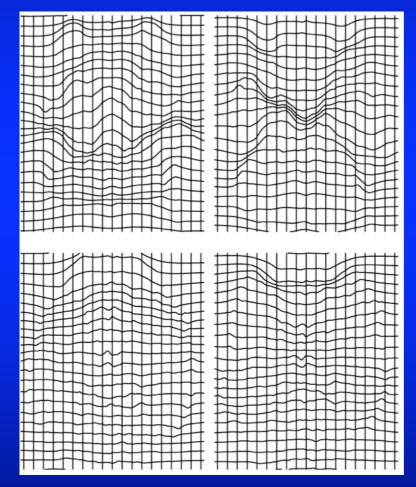


Compute nonlinear diffeomorphic mass-preserving registration and apply it to a regular grid

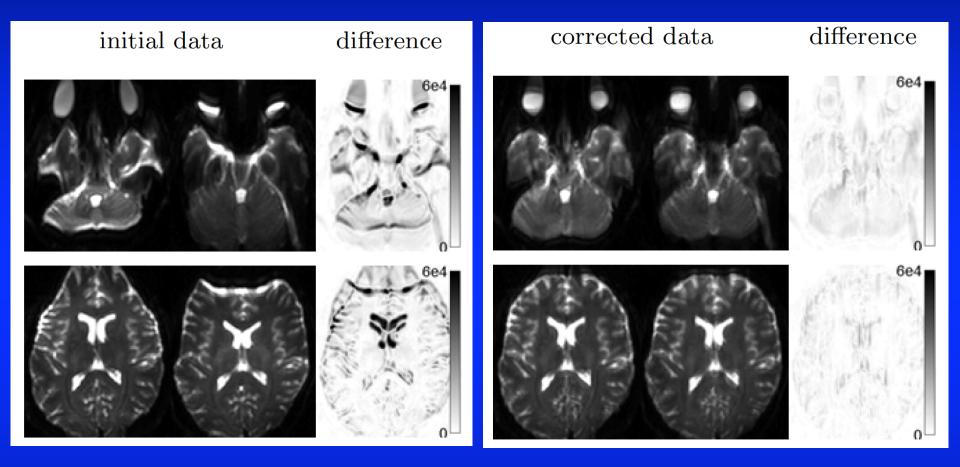
initial data







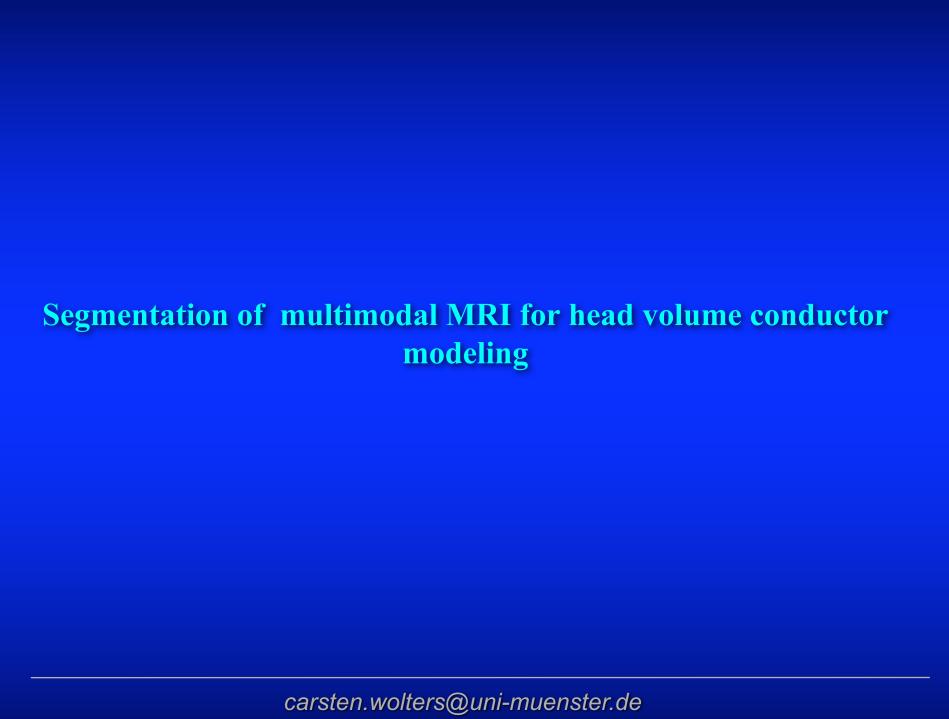
Apply registration to initial data for correction



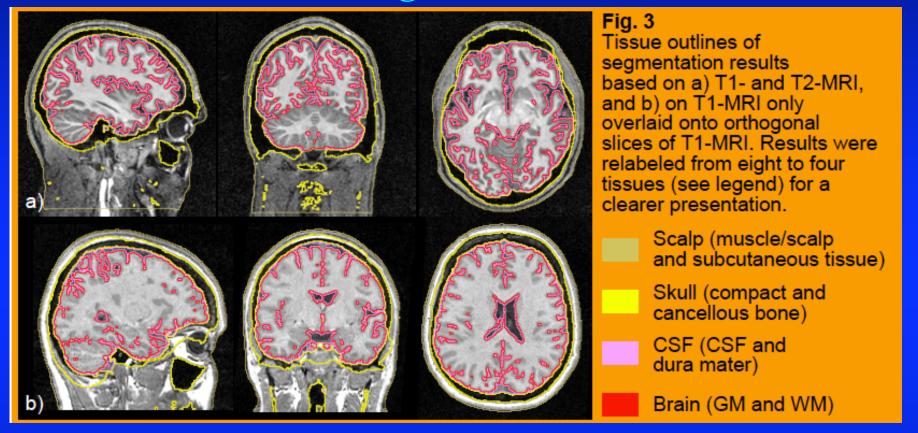
Software for registration of multimodal MRI for head volume conductor modeling:

• Open source HySCO registration tool (implemented in SPM)

(http://www.diffusiontools.com/documentation/hysco.html)

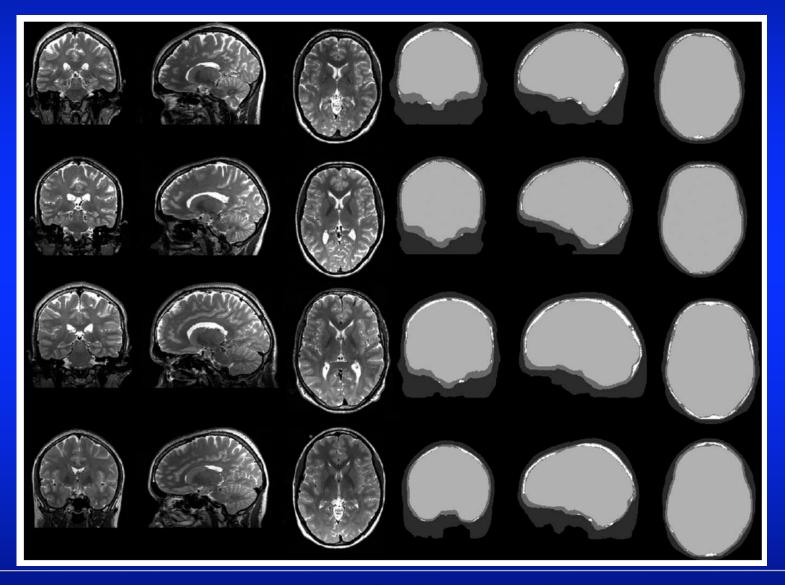


Automatic head tissue segmentation from T1- and T2-MRI



- Skin, skull, CSF and brain surfaces reconstructed from T1- and T2-MRI (Fig.3a) and only from T1-MRI (Fig.3b)
- Accurate and quasi-automatic segmentation of major head tissue compartments
- Accurate skull segmentation is especially important for applications in bioelectromagnetism

Modeling skull compacta and spongiosa



[Lanfer, PhD thesis in Mathematics, WWU Münster, 2014]

Software for segmentation of multimodal MRI for head volume conductor modeling:

- Open source SPM12 toolbox for multi-compartment segmentation: http://www.fil.ion.ucl.ac.uk/spm/software/spm12
- Open source Seg3D toolbox: Compacta and spongiosa segmentation and manual correction: http://www.sci.utah.edu/cibc-software/seg3d.html
- Open source Freesurfer toolbox for segmentation of grey matter: http://surfer.nmr.mgh.harvard.edu
- Open source FSL toolbox for segmentation of skin, skull, brain: http://www.fmrib.ox.ac.uk/fsl
- Open source SIMNIBS toolbox: http://simnibs.de/
- Lanfer-dissertation resulted in user-friendly, but commercialized, BESA-MRI pipeline: http://www.besa.de/products/besa-mri/besa-mri-overview/

Head tissue conductivity modeling

Influence of white matter conductivity

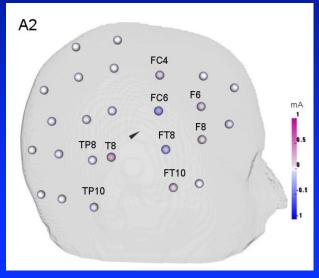
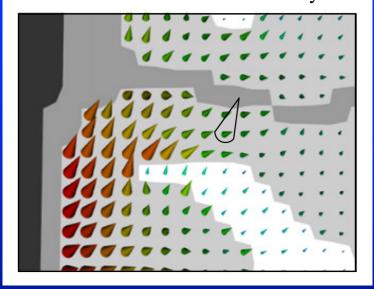


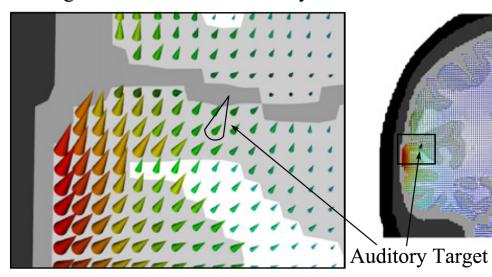
Table 2. Sensitivity of the stimulation amplitudes of the main electrodes with respect to the uncertainty in each tissue type and the stochastic interactions for the conductivity of skin σ_{skin} , skull σ_{sku} gray matter σ_{qm} , and white matter σ_{wm} .

	Sensitivity on stimulation amplitude			
Parameter	T8(%)	FC6(%)	FT8(%)	
$\sigma_{\sf skin}$	5.9	7.7	4.0	
σ_{skull}	28.9	79.8	70.1	
$\sigma_{ m gm}$	16.2	6.9	13.0	
$\sigma_{ m wm}$	27.2	0.5	3.1	
$\sigma_{skin},\sigma_{skull}$	12.0	3.5	6.6	
$\sigma_{ extsf{skull}},\sigma_{ extsf{gm}}$	7.3	1.2	2.8	
$\overline{\Sigma}$	97.5	99.5	99.6	

Low white matter conductivity



High white matter conductivity



Influence of skull conductivity

Table 2. Sensitivity of the stimulation amplitudes of the main electrodes with respect to the uncertainty in each tissue type and the stochastic interactions for the conductivity of skin σ_{skin} , skull σ_{sku} gray matter σ_{qm} , and white matter σ_{wm} .

	Sensitivity on stimulation amplitude				
Parameter	T8(%)	FC6(%)	FT8(%)		
$\sigma_{\sf skin}$	5.9	7.7	4.0		
σ_{skull}	28.9	79.8	70.1		
$\sigma_{\sf gm}$	16.2	6.9	13.0		
$\sigma_{ m wm}$	27.2	0.5	3.1		
$\sigma_{\sf skin},\sigma_{\sf skull}$	12.0	3.5	6.6		
$\sigma_{ m skull}$, $\sigma_{ m gm}$	7.3	1.2	2.8		
Σ	97.5	99.5	99.6		

Parameter	F4 (%)	F2 (%)	C4 (%)	CP4 (%)
S _{skin}	16.7	16.4	17.1	15.0
S _{skull}	47.8	47.5	46.9	43.4
S _{gm}	28.1	29.4	23.0	31.4
S _{wm}	2.3	2.2	6.0	5.2
S _{skin, skull}	0.7	0.5	1.4	0.4
S _{skin, gm}	1.1	1.0	1.2	1.1
S _{skin, wm}	0.1	0.1	0.3	0.1
S _{skull, gm}	2.7	2.5	2.9	2.6
S _{skull, wm}	0.3	0.3	0.8	0.5
S _{gm, wm}	0.1	0.2	0.3	0.3

Sensitivity on TES forward problem

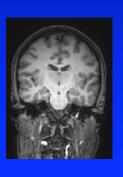
Sensitivity on EEG forward problem

Summary: Calibrated head volume conductor modeling

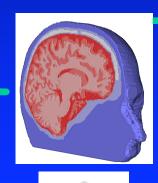
MRI measurement

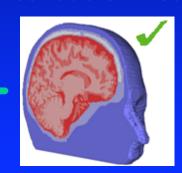
Registration Segmentation Anisotropic head model

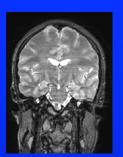
Calibrated volume conductor model

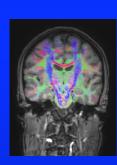


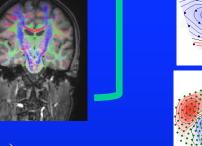


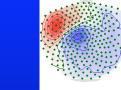












T1, T2, DTI (27 min)

Medianus-nerve SEP/SEF (7 min)

Individual skull conductivity calibration

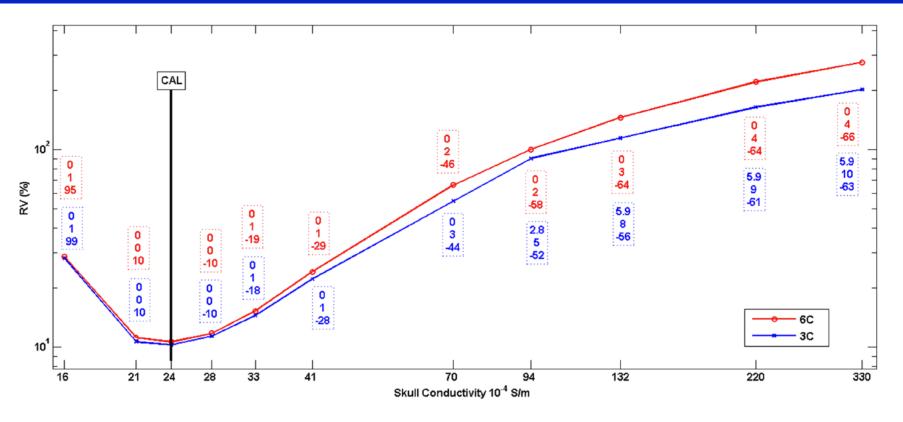


Figure 3. Skull conductivity calibration graph. RV (in %) obtained from Algorithm 2 in step 2.d. for different skull conductivity parameters for 6C (red) and 3C (blue) head models. The differences to the calibrated head models $6C_Cal$ and $3C_Cal$ (indicated by the black bar, see also Table 1) in source reconstruction are indicated by boxes with dashed frames: Difference in source location x (top row, in mm), orientation o_2 (middle row, in degree) and strength m_2 (bottom row, in %).

Individual skull conductivity calibration

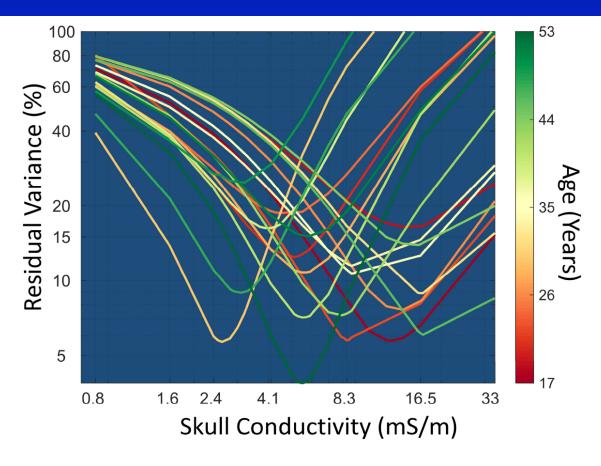


Figure 4. Skull conductivity calibration graph. Residual variance (RV in %) curves as they were estimated by the skull conductivity calibration procedure. The RV curves are presented as a function of the skull compacta conductivity for all the subjects. The horizontal axis is in mS/m and the vertical axis is in %. Each curve is color-coded by the age of the subject.

Individual skull conductivity calibration

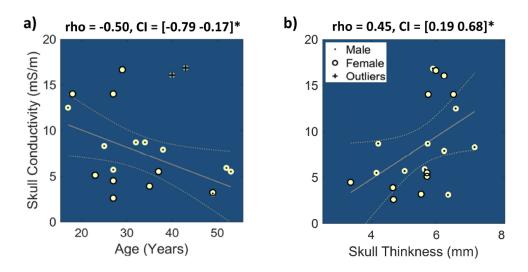


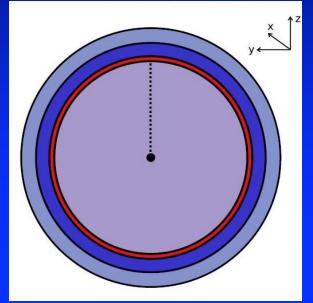
Figure 6. Interaction of skull conductivity with age and skull thickness. The current figure includes the robust correlations between the skull conductivity and a) age, or b) the full thickness of the skull (skull thickness). These two were the only correlations that exceeded the level of significance (p < 0.05). The skipped Pearson correlation value (rho) and confidence interval [CI] are presented on the top of every image. The symbol '*' denotes a significant statistical correlation (p < 0.05) between the two variables. A gray line represents the slope of the relationship and gray dashed lines represent the 95 % of CI. Markers are used for the discrimination between genders (Male: dot marker, Female: circle marker) while a third marker (black midtransparent circled cross of white color) outlines the outliers per correlation pair. The units are indicated in the vertical and horizontal axis of each plot. Namely, they are mS/m for the skull conductivity, years for the age, and mm for the skull thickness.

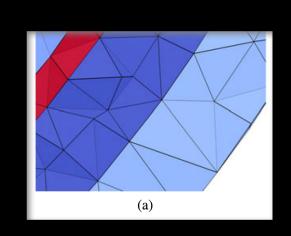
Outline

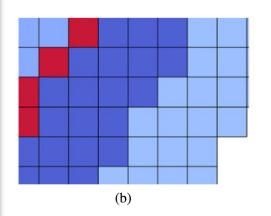
- Head model generation: MRI/DTI registration and segmentation and individual modeling of head tissue conductivities
- Forward modeling in TES and EEG: Numerical investigations
- Reconstruction: Combined EEG/MEG source analysis in presurgical epilepsy diagnosis
- Manipulation: Optimization approaches for multi-sensor tES/TMS and application to the individual stimulation of the somatosensory cortex
- Summary

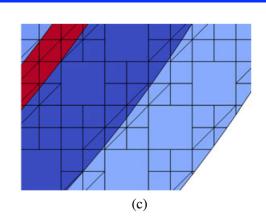
[Vogenauer, Master Thesis in Mathematics, 2019] [Piastra,..., Wolters, Frontiers in Neurosci., 2018] [Engwer, Vorwerk, Ludewig & Wolters, SIAM J. Sci. Comp., 2017]

Validation and evaluation of new FEM forward approaches









nultilayer sphere verification. From left to right, the images show the *DG-tet-1447k*, *DG-hex-3057k*, and colors represent the different conductivity values. (a) Conforming tetrahedral mesh. (b) Conforming hexahedral mesh. (c) Cut

cell mesh.

TES: Validation and evaluation of surface-based tetrahedral FEM

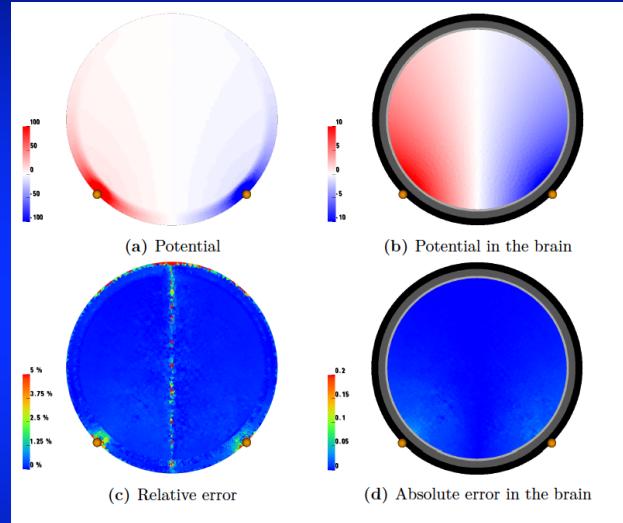
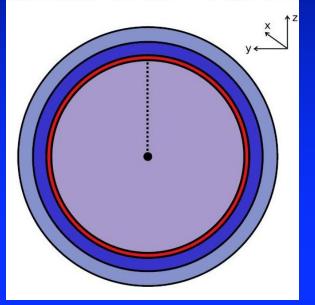
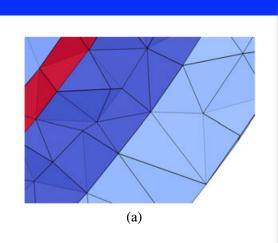
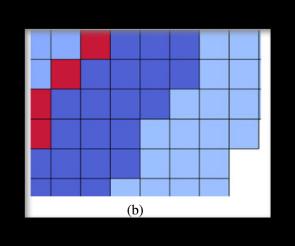


Figure 5.3.: The numerical solution in the tet-4layer-434k sphere model for tES forward problem (a) in the whole volume conductor and (b) just the brain compartment. Visualization of the (c) relative error and (d) the absolute error between numerical and analytical solution in the brain compartment.

Validation and evaluation of new FEM forward approaches







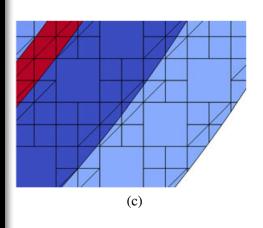
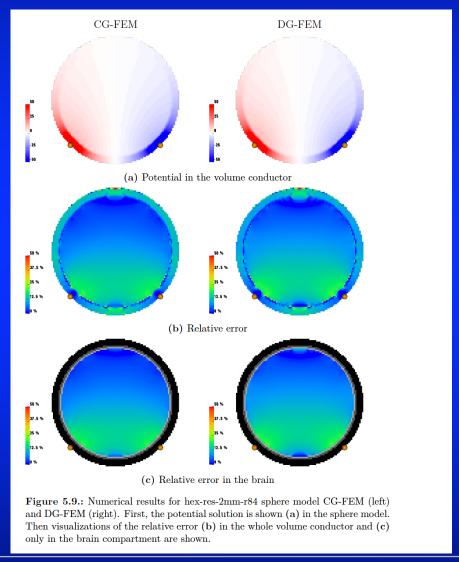


Fig. 3. Sections of the different meshes used in th

ages show the DG-tet-1447k, DG-hex-3057k, and

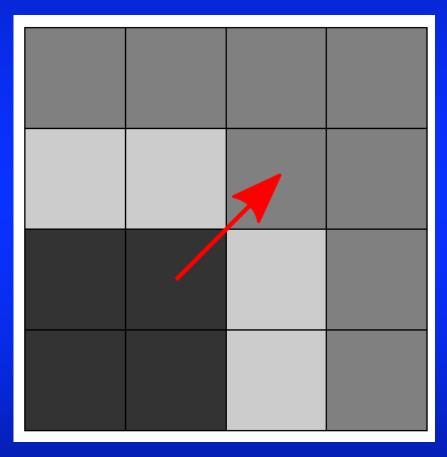
UDG-1335k models. The different colors represent the different conductivity values. (a) Conforming tetrahedral mesh. (b) Conforming hexahedral mesh. (c) Cut cell mesh.

TES: Validation of Continuous Galerkin (CG) and Discontinuous Galerkin (DG) FEM in 2 mm hexahedral meshes with 4 mm skull thickness



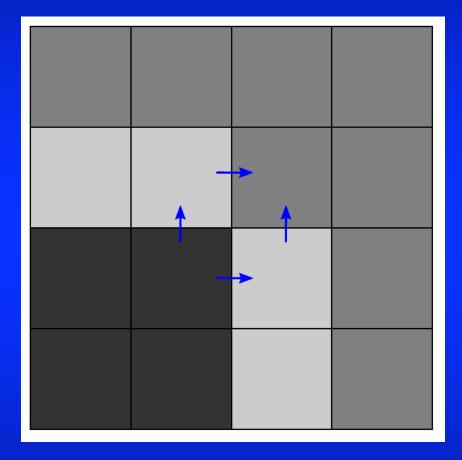
[Vogenauer, Master Thesis in Mathematics, 2019] [Piastra,..., Wolters, Frontiers in Neurosci., 2018] [Engwer, Vorwerk, Ludewig & Wolters, SIAM J. Sci. Comp., 2017]

"Skull leakages" when using standard FEM in insufficiently resolved hexahedral models



CG-FEM: Unphysical current flow through an FE node

Discontinuous Galerkin- (DG-) FEM in hexahedral models

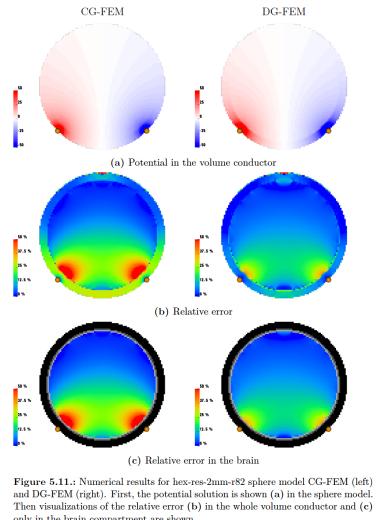


DG-FEM:

Continuous radial current flow component over tissue boundaries Discontinuous potential over tissue boundaries

[Vogenauer, Master Thesis in Mathematics, 2019] [Piastra,..., Wolters, Frontiers in Neurosci., 2018] [Engwer, Vorwerk, Ludewig & Wolters, SIAM J. Sci. Comp., 2017]

TES: Validation of Continuous Galerkin (CG) and Discontinuous Galerkin (DG) FEM in 2 mm hexahedral meshes with 2 mm skull thickness

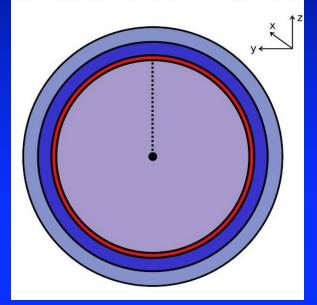


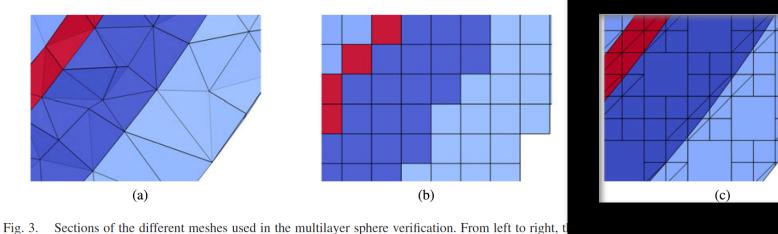
only in the brain compartment are shown.

[Vogenauer, Master Thesis in Mathematics, 2019] [Piastra,..., Wolters, Frontiers in Neurosci., 2018]

[Engwer, Vorwerk, Ludewig & Wolters, SIAM J. Sci. Comp., 2017]

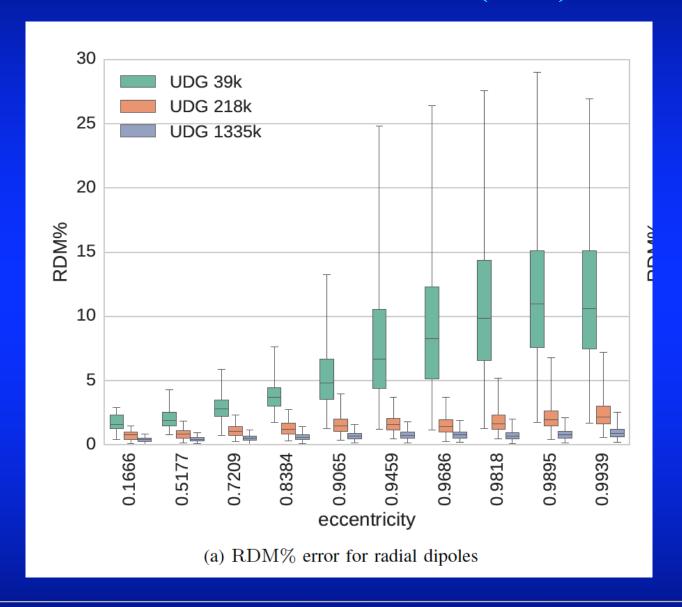
Validation and evaluation of new FEM forward approaches





UDG-1335k models. The different colors represent the different conductivity values. (a) Conforming tetrahedral mesh. (b) Conforming hexahedral mesh. (c) Cut cell mesh.

EEG: Validation of Unfitted DG (UDG) FEM



[Antonakakis, Schrader, Wollbrink, Oostenveld, Rampp, Haueisen & Wolters, *HBM*, 2019]

Guideline for volume conductor modeling

- The volume conductor model needs to contain all important tissues between the electrodes and the target brain areas
- Isotropic representations of the compartments skin, skull,
 CSF and brain grey and white matter are indispensable for any simulation
- The individual skull conductivity needs to be estimated (e.g. through SEP/SEF calibration)
- Skull compacta and spongiosa compartments should be distinguished, if a significant layer of spongiosa is between the electrodes and the targets
- White matter conductivity anisotropy modeling is important for deeper target areas

Software for FEM forward modeling:

- Freely available SimBio toolbox:
 https://www.mrt.uni-jena.de/simbio/index.php/Main_Page
- Freely available DUNEuro code: https://www.duneuro.org
- Freely available Fieldtrip-SimBio pipeline (until now only EEG):
 - [Vorwerk, Oostenveld, Magyari, Wolters, *Biomed Eng Online*, 2018] http://www.fieldtriptoolbox.org/tutorial/headmodel_eeg_fem
- Soon: Freely available Brainstorm-SimBio/DUNEuro (NIH-funded)
- Open source SimNIBS toolbox: http://simnibs.de/
- Commercial codes: BESA MRI, CURRY8

Outline

- Head model generation: MRI/DTI registration and segmentation and individual modeling of head tissue conductivities
- Forward modeling in TES and EEG: Numerical investigations
- Reconstruction: Combined EEG/MEG source analysis in presurgical epilepsy diagnosis
- Manipulation: Optimization approaches for multi-sensor tES/TMS and application to the individual stimulation of the somatosensory cortex
- Summary

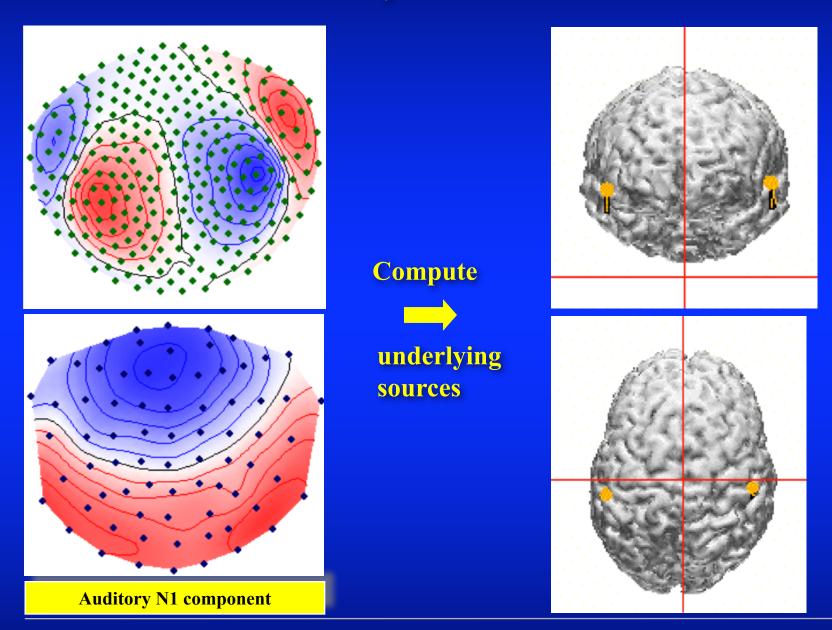
Introduction to the inverse problem in EEG and MEG source analysis

Measure combined EEG/MEG



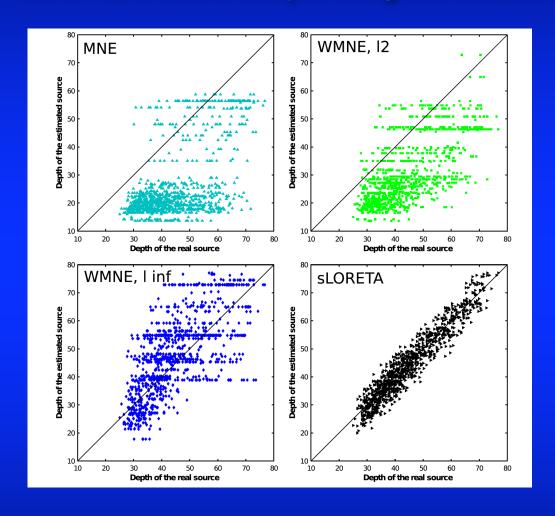
Measure auditory evoked field (AEF) and potential (AEP) when listening to sinus-tones

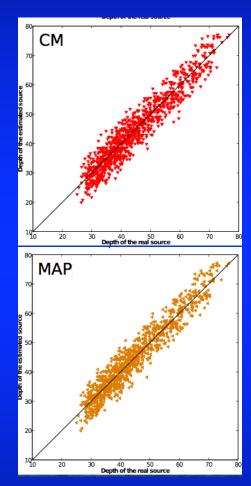
EEG/MEG source analysis



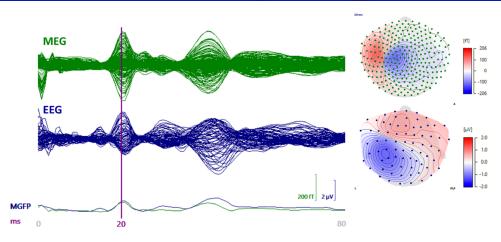
Methodological considerations for the EEG/MEG inverse problem

EEG/MEG source analysis using Hierarchical Bayesian Modeling (HBM)



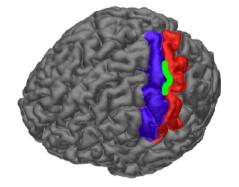


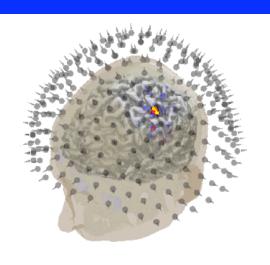
EEG/MEG source analysis using Hierarchical Bayesian Modeling (HBM)



EEG and MEG data

Fig. 3 The data obtained in the simultaneous EEG (left) and MEG (right) SEP/SEF measurements. The actual stimulus response was measured for a 100 ms interval between the pre-stimulus and post-stimulus phase. The P20-N20 component investigated in this study corresponds to the peaks corresponding to the 20 ms post-stimulus time point which is indicated by the vertical line.





Application of source analysis to presurgical epilepsy diagnosis

[Rampp, Stefan, Wu, Kaltenhäuser, Maess, Schmitt, Wolters, Hamer, Kasper, Schwab, Doerfler, Blümcke, Rössler, Buchfelder, *Brain*, 2019]



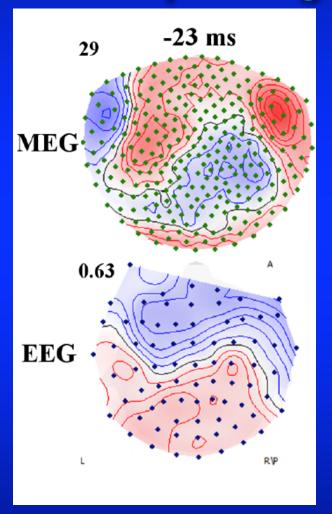
Brain

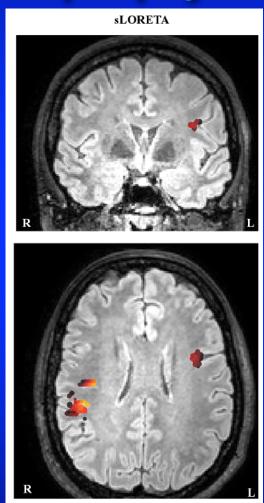
Magnetoencephalography for epileptic focus localization: A series of 1000 cases

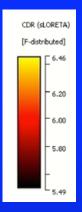
The results show that MEG provides non-redundant information, which significantly contributes to patient selection, focus localization and ultimately long-term seizure freedom after epilepsy surgery.

Specifically in extra-temporal lobe epilepsy and non-lesional cases, MEG provides excellent accuracy.

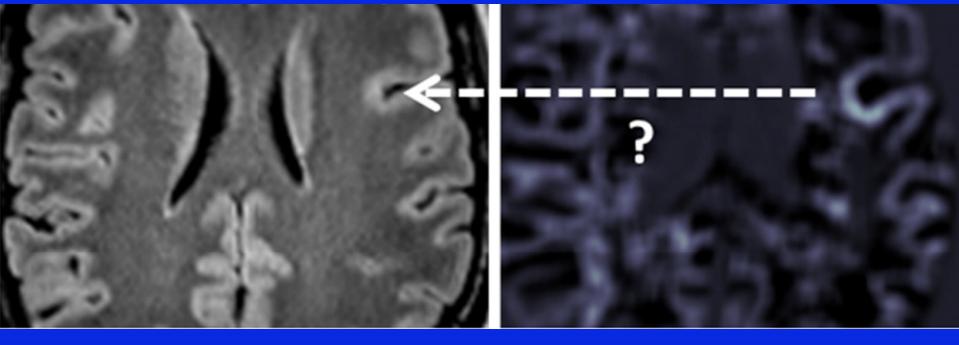
Combined EEG/MEG source analysis in presurgical epilepsy diagnosis







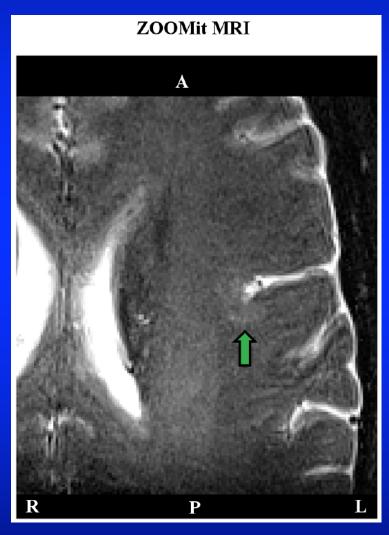
3T MRI (3D-FLAIR) and morphometric analysis



Even retrospectively in 3D-FLAIR nearly not visible left supra-insular FCD...

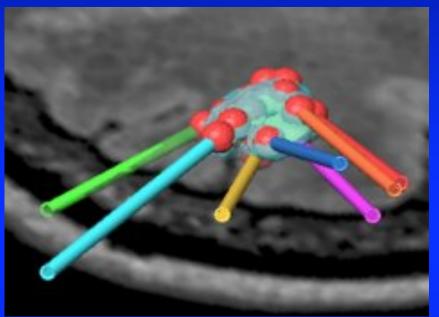
...that could also only weakly be confirmed by morphometric analysis (MAP07: Huppertz et al., 2005)...

ZOOMit MRI in localized (at -23 ms) ROI (radiological convention)



...and which was hard to see even in T2 ZOOMit

Radio-frequency thermo-coagulation (RFTC)





Lesion guided stereotactic radiofrequency thermocoagulation for palliative, in selected cases curative epilepsy surgery



Jörg Wellmer ^{a,*}, Yaroslav Parpaley ^b, Stefan Rampp ^{a,c}, Stoyan Popkirov ^a, Harald Kugel ^d, Ümit Aydin ^e, Carsten H. Wolters ^e, Marec von Lehe ^b, Jürgen Voges ^{f,g}

- ^a Ruhr-Epileptology, Department of Neurology, University Hospital Knappschaftskrankenhaus, In der Schornau 23-25, 44892 Bochum, Germany
- ^b Department of Neurosurgery, University Hospital Knappschaftskrankenhaus, In der Schornau 23-25, 44892 Bochum, Germany
- ^c Department of Neurosurgery, University of Erlangen, Schwabachanlage 6, 91054 Erlangen, Germany
- ^d Department of Clinical Radiology, University Hospital M\u00fcnster, Albert-Schweitzer-Campus 1, 48149 M\u00fcnster, Germany
 ^e Institute for Biomagnetism and Biosignalanalysis, Westfalian Wilhelms-University M\u00fcnster, Malmedyweg 15, 48149 M\u00fcnster, Germany
- f Department of Stereotactic Neurosurgery, Otto-von-Guericke University, Leipziger Str. 44, 39120 Magdeburg, Germany
- ² Leibniz Institute for Neurobiology, Brenneckestraße 6, 39118 Magdeburg, Germany

Patient got RFTC in left fronto-central FCD and surgical outcome supported our diagnosis

Software for EEG/MEG source analysis:

- Freely available SimBio toolbox:
 https://www.mrt.uni-jena.de/simbio/index.php/Main_Page
- Freely available Fieldtrip toolbox: http://www.fieldtriptoolbox.org
- Freely available Brainstorm toolbox:
 http://neuroimage.usc.edu/brainstorm
- Freely available MNE toolbox:
 https://martinos.org/mne/stable/index.html
- Commercial tools such as BESA or CURRY

Outline

- Head model generation: MRI/DTI registration and segmentation and individual modeling of head tissue conductivities
- Forward modeling in TES and EEG: Numerical investigations
- Reconstruction: Combined EEG/MEG source analysis in presurgical epilepsy diagnosis
- Manipulation: Optimization approaches for multi-sensor tES/TMS and application to the individual stimulation of the somatosensory cortex
- Summary

Hardware for transcranial electric stimulation (tES)



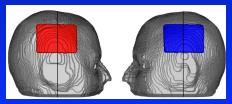
• Standard hardware for tES are two electrode patches, one anode and one cathode, used in many studies

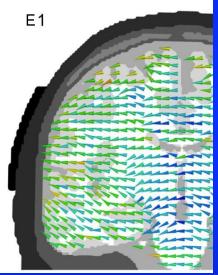


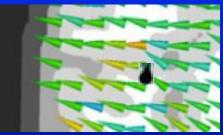
• However, first multi-electrode tES hardware and electrode optimization approaches exist, bearing the potential for much improved effects (see, e.g., Dmochowski et al., 2011,2013; Sadleir et al., 2012; Ruffini et al., 2014; Fernandez-Corazza et al., 2016; Wagner et al., 2016)

Simulation of auditory tES

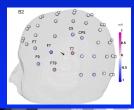
Standard two-patch

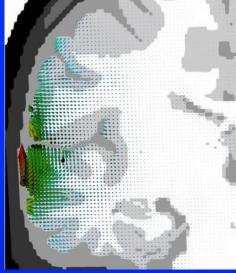






10/10 system electrodes







- Individual targeting: Electric field should be
 - maximal in area of interest
 - minimal in other areas
 - oriented radially-inwards to target cortex (Creutzfeldt et al., 1962; Krieg et al., 2013,2015; Seo, PhD thesis, 2016)

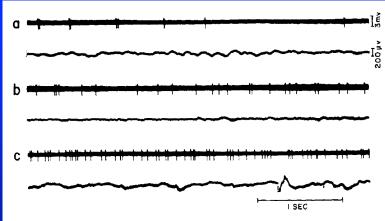
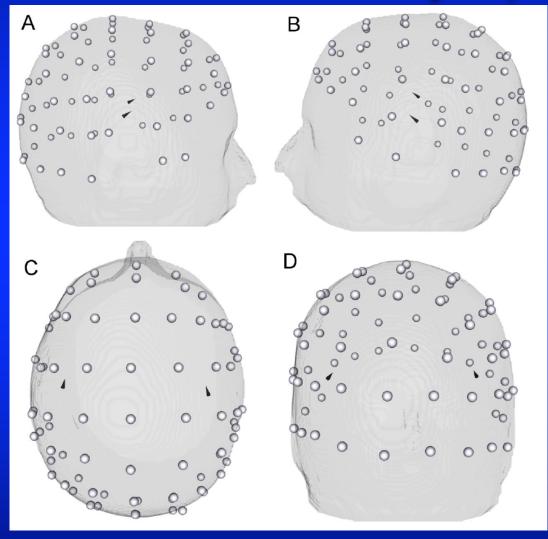
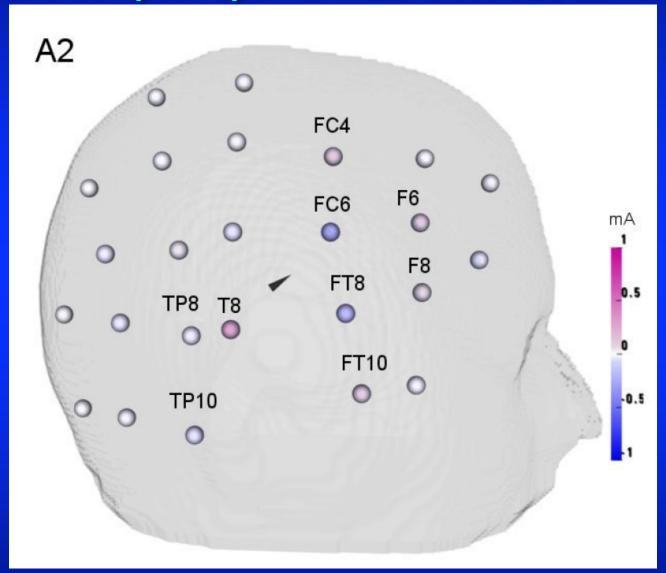


Fig. 2. Effect of transcortical d-c current on spontaneous neuron activity and EEG in the optic cortex; a, 500 μ outward (surface-negative); b, control; c, 500 μ inward (surface-positive).

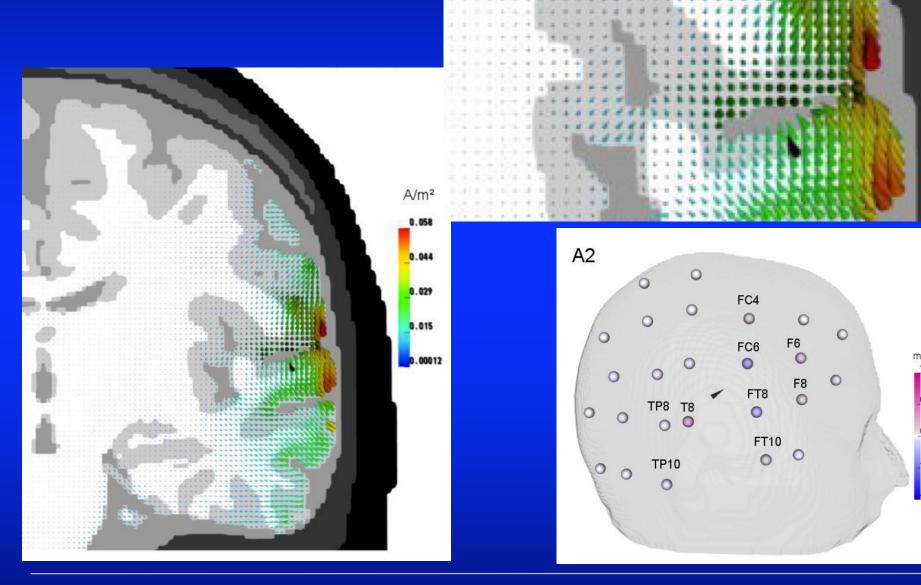
Use individualized head model and targets (here: sources of auditory N1)...



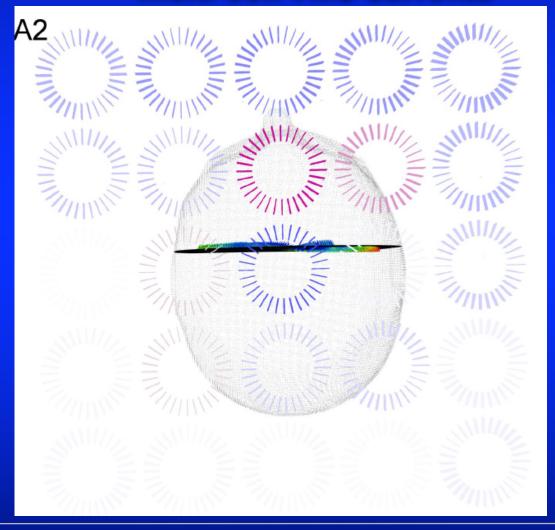
... and compute optimal multi-electrode currents...



...that lead to optimally-targeted brain currents



Mathematics are similar for multi-coil TMS: Use head model and targets. Software then computes optimal multi-coil TMS currents





Evaluation of TES optimization based on CG- and DG-FEM

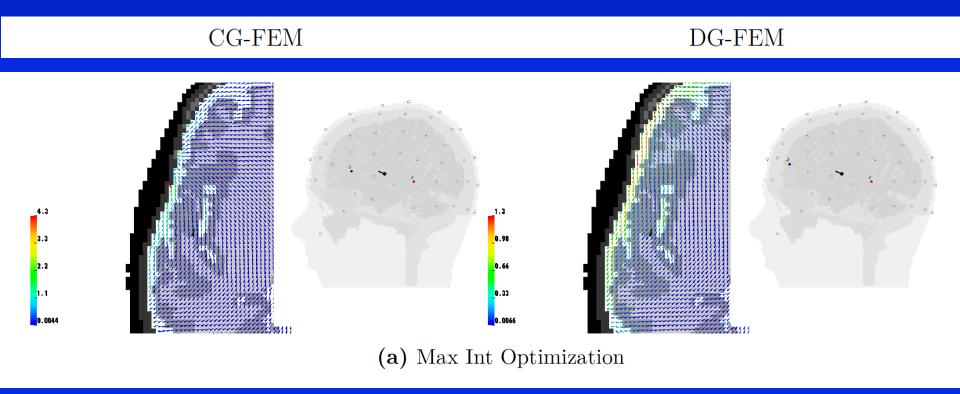


Figure 6.5.: Visualization using (a) max int optimization (b) penalized max int optimization and (c) optimization using ADMM for the numerical approaches CG-FEM and DG-FEM in the realistic head model with 2mm resolution for an auditory target. Note that here the scaling of the current density magnitude is different in the different plots.

Evaluation of TES optimization based on CG- and DG-FEM

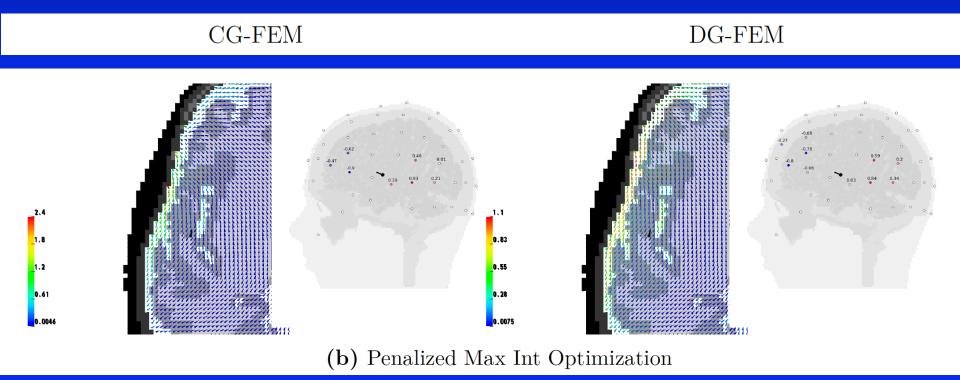


Figure 6.5.: Visualization using (a) max int optimization (b) penalized max int optimization and (c) optimization using ADMM for the numerical approaches CG-FEM and DG-FEM in the realistic head model with 2mm resolution for an auditory target. Note that here the scaling of the current density magnitude is different in the different plots.

Evaluation of TES optimization based on CG- and DG-FEM

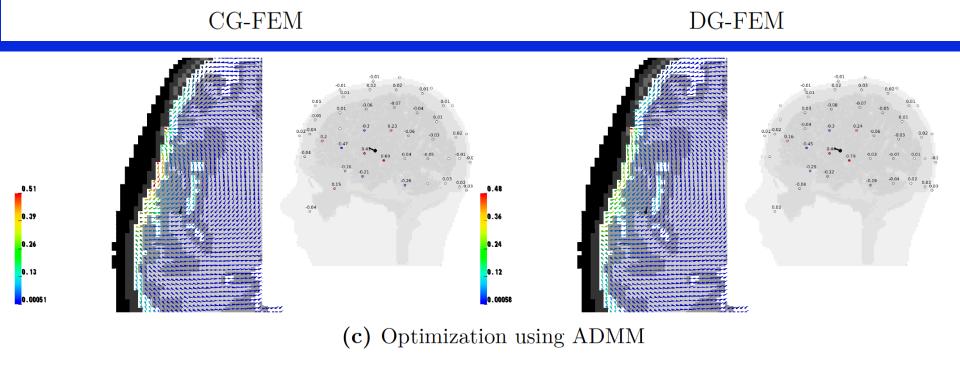


Figure 6.5.: Visualization using (a) max int optimization (b) penalized max int optimization and (c) optimization using ADMM for the numerical approaches CG-FEM and DG-FEM in the realistic head model with 2mm resolution for an auditory target. Note that here the scaling of the current density magnitude is different in the different plots.

Individualized and optimized multi-channel TES for drug-resistant epilepsy patient where resection was refused due to proximity of FCD to eloquent cortex (Broca)

Individualized and optimized multi-channel TES for drugresistant epilepsy patient

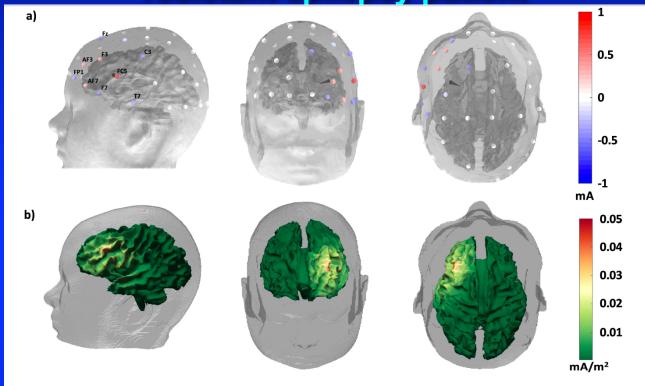


Fig. 4. The present figure includes **a**) the optimized tDCS montage and **b**) the current density distribution for the patient. The channels are colored by the simulated injected currents ranging from -1 up to 1 mA. The total sum of the currents in the electrodes is equal to 2 mA. The colored brain surface of the patient represents the distribution of the current density measured in mA/m². The black cone represented the target of the tDCS stimulation simulation.

Software for optimized multi-electrode TES and multi-coil TMS:

- Matlab-code for optimization (PhD theses of Sven Wagner/Asad Khan, Master theses of Simon Homölle/Nikolas Vogenauer)
- Optimizer calls freely available DUNEuro toolbox for TES forward modeling (Master theses of Simon Homölle/Nikolas Vogenauer): https://www.duneuro.org
- Optimizer calls freely available SimBio toolbox for TES/TMS forward modeling (PhD theses of Sven Wagner): https://www.mrt.uni-jena.de/simbio/index.php/Main_Page

Outline

- Literature
- Head model generation: MRI/DTI registration and segmentation and individual modeling of head tissue conductivities
- Forward modeling in TES and EEG: Numerical investigations
- Reconstruction: Combined EEG/MEG source analysis in presurgical epilepsy diagnosis
- Manipulation: Optimization approaches for multi-sensor tES/TMS and application to the individual stimulation of the somatosensory cortex
- Summary

Summary

- EEG/MEG contain complementary information so that combined EEG/MEG source analysis offers accurate reconstruction of both source locations and orientations -> Improved setup of targets for multi-sensor TES/TMS (Aydin et al., 2014, 2015, 2017; Antonakakis et al., 2019; Khan et al., 2019)
- Inverse multi-sensor TES/TMS problem: Optimized targeting bears potential for improvement of effects (Dmochowski et al., 2011,2013; Sadleir et al., 2012; Ruffini et al., 2014; Schmidt et al., 2015; Wagner et al., 2016; Baltus et al., 2018; Antonakakis et al., 2019; Khan et al., 2019)
- Forward multi-sensor TES/TMS problem:
 - Finite element method (FEM) based calibrated realistic (6CA) head modeling is important and optimized processing pipelines are needed (Windhoff et al., 2011; Ruthotto et al., 2012; Lanfer et al., 2013; Miranda et al., 2013; Aydin et al., 2014,2015; Opitz et al., 2015; ; Antonakakis et al., 2019; Khan et al., 2019)
 - With unfitted FEM we avoid numerical artifacts and achieve best numerical accuracy in realistic head models without topological restrictions, while avoiding complicated FEM meshing strategies (Nüßing, PhD thesis, 2018; Nüßing et al., IEEE TBME, 2016; Engwer et al., SIAM Sci. Comp., 2017)

Thank you for your attention!





Since 2016



2010-2016



Münster SIM-NEURO workgroup